

# Circ-PRKDC Facilitates the Progression of Colorectal Cancer Through miR-198/DDR1 Regulatory Axis

This article was published in the following Dove Press journal:  
*Cancer Management and Research*

Guixiang Wang<sup>1</sup>  
Yajun Li<sup>1</sup>  
Hufei Zhu<sup>1</sup>  
Guoqiang Huo<sup>1</sup>  
Jingying Bai<sup>1</sup>  
Zhiyong Gao<sup>2</sup>

<sup>1</sup>Department of Colorectal Surgery, Yan'an People's Hospital, Yan'an, Shaanxi, People's Republic of China; <sup>2</sup>Department of General Surgery, Yanchuan County People's Hospital, Yan'an, Shaanxi, People's Republic of China

**Background:** Circular RNAs (circRNAs) play a crucial role in a variety of cancers, including colorectal cancer (CRC). This study aimed to explore the role of *hsa\_circ\_0136666* (*circ-PRKDC*) in CRC and its potential mechanism.

**Methods:** The levels of *circ-PRKDC*, *miR-198* and discoidin domain receptor 1 (*DDR1*) were measured using quantitative real-time polymerase chain reaction or Western blot. Cell viability was detected using cell counting kit-8 (CCK-8) assay. Cell apoptosis and cycle were evaluated via flow cytometry. Cell migration and invasion were examined using transwell assay. CyclinD1 protein level was determined via Western blot. The interaction among *circ-PRKDC*, *miR-198* and *DDR1* was confirmed by dual-luciferase reporter assay and RNA immunoprecipitation assay. Xenograft assay was performed to analyze tumor growth in vivo.

**Results:** *Circ-PRKDC* and *DDR1* levels were increased, and *miR-198* level was decreased in CRC tissues and cells. *Circ-PRKDC* depletion inhibited proliferation, migration and invasion, and expedited apoptosis and cell cycle arrest in SW480 and HCT116 cells. Silence of *circ-PRKDC* impeded CRC progression by sponging *miR-198*. Overexpression of *miR-198* hindered CRC development via targeting *DDR1*. Moreover, *circ-PRKDC* silencing suppressed tumor growth in vivo.

**Conclusion:** Knockdown of *circ-PRKDC* inhibited CRC progression via modulating *miR-198/DDR1* pathway.

**Keywords:** colorectal cancer, *circ-PRKDC*, *miR-198*, *DDR1*, cell cycle

## Introduction

Colorectal cancer (CRC) is one of the most common malignant tumors in the world.<sup>1</sup> CRC has caused 1.8 million new cases and 881,000 deaths in 2018, resulting in CRC ranking third in cancer incidence and second in mortality.<sup>2</sup> Surgery accompanied by adjuvant chemotherapy and radiotherapy is the first choice for CRC patients.<sup>3,4</sup> Nevertheless, the prognosis of CRC remains unsatisfactory, especially in metastatic patients.<sup>5</sup> Therefore, discovering novel biomarkers for CRC diagnosis and treatment is urgent.

Circular RNA (circRNA) has a covalent closed-loop structure and no 5' to 3' polarity, which is different from linear RNA.<sup>6</sup> CircRNAs exert a critical effect on tumorigenesis and metastasis by acting as microRNA (miRNA) sponges.<sup>7</sup> For example, *circRBM33* expedited the malignant behaviors of gastric cancer via absorbing *miR-149* to elevate *IL-6* level.<sup>8</sup> In breast cancer, *circRNA\_002178* contributed to energy metabolism and angiogenesis by sponging *miR-328-3p*.<sup>9</sup>

Correspondence: Zhiyong Gao  
Tel +86-911-2888754  
Email diavze@163.com

In addition, plentiful studies have demonstrated that circRNAs participate in the occurrence and development of CRC and are promising biomarkers for CRC diagnosis and prognosis.<sup>10</sup> In 2019, Jin et al revealed that *hsa\_circ\_0136666* derived from DNA-Dependent Protein Kinase Catalytic Subunit (*PRKDC*) was overtly up-regulated in CRC through circRNA high-throughput sequencing.<sup>11</sup> Chen et al revealed that *circ-PRKDC* enhanced 5-Fluorouracil resistance in CRC via absorbing *miR-375* to up-regulate *FOXM1* through Wnt/ $\beta$ -catenin pathway.<sup>12</sup> Moreover, Liu et al suggested that *circ-PRKDC* expedited the malignant behaviors of CRC via competitively binding to *miR-1299* and activating *CDK6*.<sup>13</sup> Nevertheless, the precise mechanism of *circ-PRKDC* in CRC needs further investigation.

Increasing evidence has illuminated that miRNAs were aberrantly expressed in various cancers and participate in tumor occurrence and development via mediating a range of genes and signaling pathways.<sup>14,15</sup> Moreover, a large number of miRNAs are related to CRC process.<sup>16</sup> For instance, *miR-365a-3p* overexpression blocked CRC cell progression by targeting *ADAM10* and regulating JAK/STAT pathway.<sup>17</sup> Additionally, *miR-1224-5p* restrained CRC cell metastasis via modulating *SPI*-triggered NF- $\kappa$ B signaling.<sup>18</sup> Also, *miR-144-3p* functioned as a tumor-suppressing factor in CRC through regulation of *BCL6*/Wnt/ $\beta$ -catenin pathway.<sup>19</sup> In previous research, *miR-198* level was prominently decreased in CRC.<sup>20</sup> Furthermore, Li et al suggested that *miR-198* hindered CRC cell progression via inhibiting *ADAM28* and blocking JAK/STAT pathway.<sup>21</sup> Nevertheless, the association between *circ-PRKDC* and *miR-198* has not been studied.

Discoidin domain receptor 1 (*DDR1*) is classified as receptor tyrosine kinases family and is activated by binding to collagen.<sup>22</sup> Mounting evidence has demonstrated that *DDR1* possesses the characteristics of maintaining cell differentiation and promoting cell metastasis.<sup>23</sup> Recently, *DDR1* has been verified to be dysregulated in various tumors, including oral cancer,<sup>24</sup> triple-negative breast cancer<sup>25</sup> and thyroid cancer.<sup>26</sup> Also, Sirvent et al revealed that depletion of *DDR1* contributed to the treatment of metastatic CRC.<sup>27</sup> In addition, we discovered that *miR-198* might target *DDR1* based on bioinformatics analysis. However, whether the targeting relationship exists or plays a role in CRC is unknown.

Herein, we studied the function of *circ-PRKDC* in CRC cell progression. Furthermore, we unveiled that *circ-PRKDC/miR-198/DDR1* axis may provide a novel therapeutic approach for CRC therapy.

## Materials and Methods

### Specimen Collection

All clinical samples, including CRC tissues (n=30) and matched adjacent non-tumor tissues (n=30), were obtained from 30 patients with CRC who underwent resection surgery at Yan'an People's Hospital. Non-tumor colorectal tissues were sampled at least 5 cm distal to the tumor, and all tissues were subjected to histological examination. After snap-freezing with liquid nitrogen, all specimens were stored at  $-80^{\circ}\text{C}$ . This procedure was ratified by the Ethics Committee of Yan'an People's Hospital. Written informed consent was collected from all participants. The inclusion criteria were as follows: the subject was diagnosed with CRC and had no history of other tumors; no chemotherapy or radiotherapy prior to surgery; clinical data were complete. The pathological features of CRC patients are presented in Table 1.

### Cell Culture

CRC cell lines (SW480 and HCT116) and normal colonic epithelial cell line (FHC) were commercially acquired from American Type Culture Collection (ATCC, Manassas, VA, USA). All cells were cultured in RPMI-1640 medium (Hyclone, Logan, UT, USA) supplemented with 10% fetal bovine serum (FBS; Hyclone) at  $37^{\circ}\text{C}$  with 5%  $\text{CO}_2$ .

### Cell Transfection

*Circ-PRKDC* small interfering RNA (si-circ-PRKDC) and negative control (si-NC), *miR-198* mimics (miR-198) and

**Table 1** Correlation Between Circ-PRKDC Expression and Pathological Features of CRC Patients

Parameters	No. of Cases	circ-PRKDC		P-value
		Low (15)	High (15)	
Ages (years)				
<60	10	6	4	0.4386
$\geq 60$	20	9	11	
Gender				
Male	13	8	5	0.269
Female	17	7	10	
TNM stage				
I+II	13	10	3	0.0099
III+IV	17	5	12	
MSI status				
MSS	13	7	6	0.7125
MSI	17	8	9	

negative control (miR-NC), *circ-PRKDC* or *DDR1* over-expression vector (*circ-PRKDC* or *DDR1*) and negative control (pcDNA), *miR-198* inhibitor (anti-miR-198) and negative control (anti-miR-NC) were synthesized from Ribobio (Guangzhou, China). Cell transfection was carried out using Lipofectamine 3000 (Invitrogen, Carlsbad, CA, USA) when cell confluence reached ~80%. After 48 h of transfection, cells were harvested for subsequent experiments.

## Quantitative Real-Time Polymerase Chain Reaction (qRT-PCR)

RNA was extracted using Trizol reagent (Solarbio, Beijing, China). Then, complementary DNA was synthesized via the specific Reverse Transcription kit (Takara, Dalian, China). Subsequently, qRT-PCR was conducted using SYBR Green PCR Master Mix (LMAI Bio, Shanghai, China). The relative expression was calculated via the  $2^{-\Delta\Delta Ct}$  method. The primers included: *circ-PRKDC*-F: 5'-CAGAGACGATTGGCTGGTGA-3', *circ-PRKDC*-R: 5'-TGATAAATTGCCCAACAAAGAGACT-3'; *miR-198*-F: 5'-GGTCCAGAGGGGAGAT-3', *miR-198*-R: 5'-GAATACCTCGGACCCTGC-3'; *DDR1*-F: 5'-CTTCAGCGAAATCTCCTTCATC-3', *DDR1*-R: 5'-CCAACACCTCCGTTTCAGCCT-3'; *GAPDH*-F: 5'-GGGAAACTGTGGCGTGAT-3', *GAPDH*-R: 5'-GAGTGGGTGTCGCTGTTGA-3'; *U6*-F: 5'-CTCGCTTCGGCAGCACA-3', *U6*-R: 5'-AACGCTTCACGAATTTGCGT-3'. *GAPDH* or *U6* was regarded as an internal reference.

## Cell Viability Assay

Cells were seeded into 96-well plates at a density of  $5 \times 10^3$  cells per well and incubated at 37°C for 48 h. Briefly, the medium was replaced with fresh medium containing 10  $\mu$ L cell counting kit-8 (CCK-8) solution (Solarbio). After 4 h of culture, the absorbance was measured using a Microplate Reader (BioTek, Burlington, VT, USA).

## Cell Apoptosis Assay

Cell apoptosis was examined using Annexin V-FITC/Propidium Iodide (PI) Apoptosis Detection kit (Invitrogen). In brief, the transfected cells were washed twice with PBS and resuspended with binding buffer. Subsequently, the suspension was reacted with Annexin V-FITC and PI in the dark for 15 min. Next, the apoptosis rate was evaluated using a Flow Cytometer (Beckman Coulter, Miami, FL, USA).

## Transwell Assay

Cell migration and invasion were determined using transwell chambers with 8  $\mu$ m polycarbonate membrane filters (Corning, Corning, NY, USA). For cell migration test, the cells ( $5 \times 10^4$  cell/well) were seeded into the upper chamber. Additionally, the medium containing 10% FBS was placed in the lower chamber as a chemical attractant. After 24 h of incubation, the cells in the upper surface were removed with cotton swabs, and the cells in the lower surface were stained with 0.5% crystal violet. After washing twice with PBS, the migrated cells were counted in five randomly chosen fields under a microscope at a magnification of 100 $\times$ . For cell invasion test, the transwell chamber was pre-coated with Matrigel (Corning).

## Cell Cycle Assay

Cells were trypsinized and suspended in PBS after different treatments. Then, the precipitate harvested by centrifugation was resuspended in PBS. Subsequently, the cells were fixed with 70% ethanol at 4°C for 24 h and stained with 1% PI containing RNase at 4°C for 30 min. Finally, the cell cycle distribution was examined via a Flow Cytometer (Beckman Coulter).

## Western Blot Assay

Protein was extracted using RIPA lysis buffer (Solarbio). Subsequently, the equal amount of protein was separated by polyacrylamide gel electrophoresis and transferred onto polyvinylidene difluoride membranes (Millipore, Billerica, MA, USA). After being blocked with 5% non-fat milk, the membranes were probed with primary antibodies against CyclinD1 (1:1500, ab226977; Abcam, Cambridge, UK), *DDR1* (1:2000, ab227195; Abcam) or *GAPDH* (1:2500, ab9485; Abcam) at 4°C overnight. Next, the membranes were incubated with the secondary antibody (1:20000; ab205718, Abcam) at room temperature for 2 h. Finally, the signal intensity was visualized via an ECL reagent (Solarbio).

## Dual-Luciferase Reporter Assay

The fragment of *circ-PRKDC* or *DDR1* 3'UTR was cloned into the pmirGLO vector (LMAI Bio) to form WT-*circ-PRKDC* or WT-*DDR1* 3'UTR reporter. The mutant luciferase reporter vector (MUT-*circ-PRKDC* or MUT-*DDR1* 3'UTR) was constructed through mutation of *miR-198* binding sequence. Then, the corresponding vector was introduced into SW480 and HCT116 cells together with

miR-198 or miR-NC. The luciferase intensity was detected via Dual-Lucy Assay Kit (Solarbio).

## RNA Immunoprecipitation (RIP) Assay

RIP analysis was carried out using EZ-Magna RIP kit (Millipore). After lysing SW480 and HCT116 cells with RIP lysis buffer, cell lysates reacted with magnetic beads combined with Ago2 antibody or IgG antibody at 4°C. Finally, the precipitated RNA was purified and quantified by qRT-PCR.

## Xenograft Assay

The animal experiment was approved by the Animal Ethics Committee of Yan'an People's Hospital and conducted in accordance with the Guide for the Care and Use of Laboratory Animals of the National Institutes of Health. Lentivirus carrying sh-circ-PRKDC or sh-NC purchased from GenePharma (Shanghai, China) was transfected into SW480 cells.  $5 \times 10^6$  stably transfected cells were subcutaneously injected into the right abdomen of BALB/c nude mice at 5 weeks of age. Tumor volume was measured every 4 days. After 31 days, the mice were sacrificed and the tumors were weighed. The levels of *circ-*

*PRKDC*, *miR-198* and *DDR1* were examined using qRT-PCR or Western blot.

## Statistical Analysis

Data were displayed as mean  $\pm$  standard deviation. The differences were calculated using Student's *t*-test or one-way analysis of variance through GraphPad Prism 7 software (GraphPad Inc., La Jolla, CA, USA). The linear relationship of *circ-PRKDC*, *miR-198* and *DDR1* in CRC tissues was assessed via Spearman correlation coefficient.  $P < 0.05$  was considered statistically significant.

## Results

### Circ-PRKDC Level is Increased in CRC Tissues and Cells

According to previous studies, we first examined the expression of *circ-PRKDC* in CRC tissues and adjacent non-tumor tissues. The results illustrated that *circ-PRKDC* level in CRC tissues was significantly increased in comparison with adjacent normal tissues (Figure 1A). Simultaneously, we detected *circ-PRKDC* expression in human normal colonic epithelial cell line FHC and CRC cells (SW480 and HCT116). qRT-PCR analysis showed a marked elevation in *circ-PRKDC* level in SW480 and

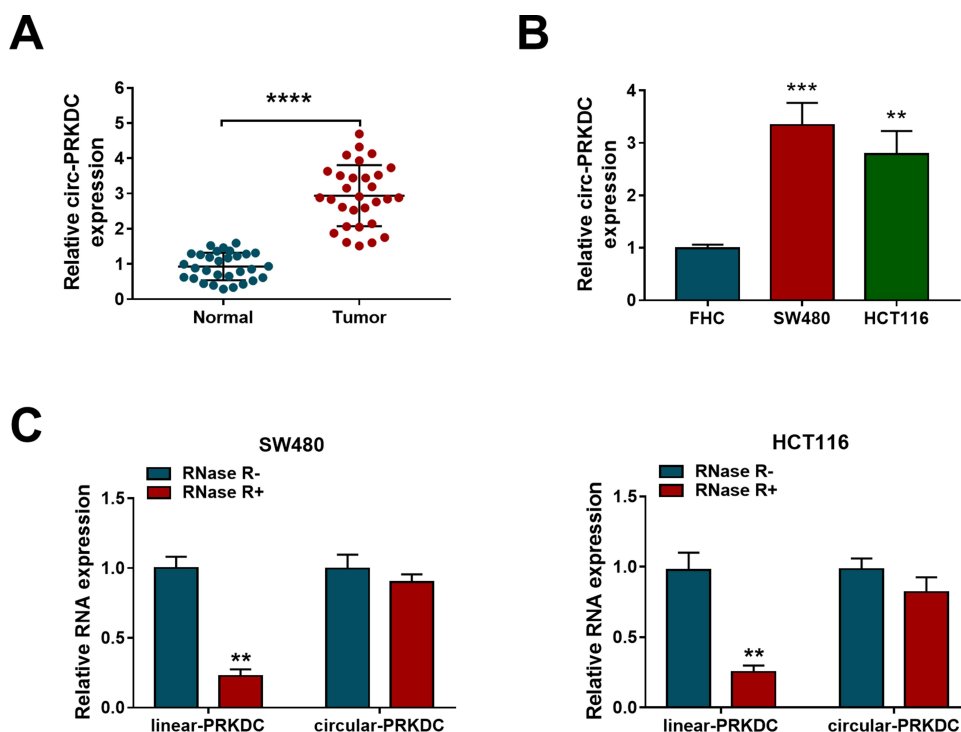


**Figure 1** Circ-PRKDC level is increased in CRC tissues and cells. (A) Expression of *circ-PRKDC* was examined in CRC tissues (n=30) and adjacent normal tissues (n=30). (B) *Circ-PRKDC* level was measured in CRC cells (SW480 and HCT116) and human normal colonic epithelial cells (FHC). (C) The levels of *circ-PRKDC* and linear *PRKDC* were detected in SW480 and HCT116 cells treated with or without RNase R. \*\* $P < 0.01$ , \*\*\* $P < 0.001$ , \*\*\*\* $P < 0.0001$ .

HCT116 cells compared with FHC cells (Figure 1B). In addition, RNase R digestion assay revealed that *circ-PRKDC* was more resistant to RNase R than linear *PRKDC* in CRC cells (Figure 1C). As shown in Table 1, *circ-PRKDC* expression was not associated with age, gender and microsatellite instability (MSI) status, but was related to TNM stage. These data indicated that *circ-PRKDC* might play a carcinogenic role in CRC.

## Circ-PRKDC Depletion Inhibits Proliferation, Migration and Invasion and Promotes Apoptosis in CRC Cells

To investigate whether *circ-PRKDC* played a carcinogenic role in CRC, si-NC or si-*circ-PRKDC* was introduced into SW480 and HCT116 cells. First, qRT-PCR assay confirmed the significant inhibition efficiency of si-*circ-PRKDC* (Figure 2A). Next, CCK-8 analysis revealed that transfection with si-*circ-PRKDC* significantly reduced the viability of SW480 and HCT116 cells (Figure 2B). Flow cytometry suggested that the apoptosis rate in the si-*circ-PRKDC* group was significantly increased compared to the control group (Figure 2C). Moreover, introduction of si-*circ-PRKDC* significantly decreased the migrated and invaded cells compared with the control group (Figure 2D and E). Besides, *circ-PRKDC* silencing led to a striking increase in the percentage of cells at G0/G1 phase and a marked decrease in the percentage of cells at S phase, indicating silence of *circ-PRKDC* induced cell cycle arrest at G0/G1 phase (Figure 2F and G). Synchronously, Western blot assay displayed a marked reduction of CyclinD1 protein level in SW480 and HCT116 cells transfected with si-*circ-PRKDC* (Figure 2H). Overall, these data indicated that knockdown of *circ-PRKDC* suppressed CRC cell proliferation, migration and invasion, and induced apoptosis.

## Circ-PRKDC Acts as a Sponge for miR-198

We speculated that *circ-PRKDC* and *miR-198* had a putative binding sequence based on Circular RNA Interactome database (<https://circinteractome.nia.nih.gov/>) (Figure 3A). To verify this prediction, we conducted a dual-luciferase reporter assay. As displayed in Figure 3B, *miR-198* mimics significantly decreased the luciferase activity of WT-*circ-PRKDC* reporter, while the effect was not significant when the binding site was mutated. Compared with adjacent non-

tumor tissues, *miR-198* level was significantly reduced in CRC tissues (Figure 3C). Similarly, *miR-198* level in SW480 and HCT116 cells was markedly lower than that in FHC cells (Figure 3D). Additionally, *circ-PRKDC* and *miR-198* levels in CRC tissues were negatively correlated (Figure 3E). Next, RIP analysis was performed to validate the binding relationship between *circ-PRKDC* and *miR-198*, and the results showed that *miR-198* and *circ-PRKDC* were enriched in Ago2 group instead of IgG group (Figure 3F and G). Then, the overexpression efficiency of *circ-PRKDC* was verified via qRT-PCR assay (Figure 3H). Moreover, knockdown of *circ-PRKDC* expedited *miR-198* expression, and up-regulation of *circ-PRKDC* restrained *miR-198* expression (Figure 3I). Collectively, these results indicated that *circ-PRKDC* directly interacted with *miR-198*.

## Inhibition of miR-198 Alleviates the Effect of Circ-PRKDC Silencing on CRC Cell Progression

To illuminate whether *circ-PRKDC* targets *miR-198* to affect CRC cell progression, a series of rescue experiments were performed in SW480 and HCT116 cells transfected with si-NC, si-*circ-PRKDC*, si-*circ-PRKDC*+anti-*miR-NC* or si-*circ-PRKDC*+anti-*miR-198*. First of all, the knockdown efficiency of *miR-198* was confirmed in CRC cells introduced with anti-*miR-NC* or anti-*miR-198* (Figure 4A). CCK-8 analysis and flow cytometry illustrated that inhibition of *circ-PRKDC* reduced cell viability and increased apoptosis of SW480 and HCT116 cells, while these changes were reversed by repressing *miR-198* (Figure 4B and C). Transwell analysis depicted that silencing of *circ-PRKDC* inhibited the migration and invasion ability of CRC cells, whereas co-transfection of si-*circ-PRKDC* and anti-*miR-198* partially alleviated these effects (Figure 4D and E). In addition, down-regulation of *circ-PRKDC* triggered G0/G1 phase arrest, which was abolished by inhibiting *miR-198* (Figure 4F and G). Also, introduction of anti-*miR-198* partially alleviated the decrease in CyclinD1 protein level caused by *circ-PRKDC* depletion (Figure 4H and I). Additionally, down-regulation of *miR-198* markedly promoted the protein expression of CyclinD1 compared with the control group (Figure S1). Thus, these results evidenced that *circ-PRKDC* knockdown impeded CRC cell progression by regulating *miR-198*.

## DDR1 is a Target of miR-198

We predicted miRNAs that might bind to *circ-PRKDC* and screened four miRNAs (*miR-198*, *miR-326*, *miR-330-5p*

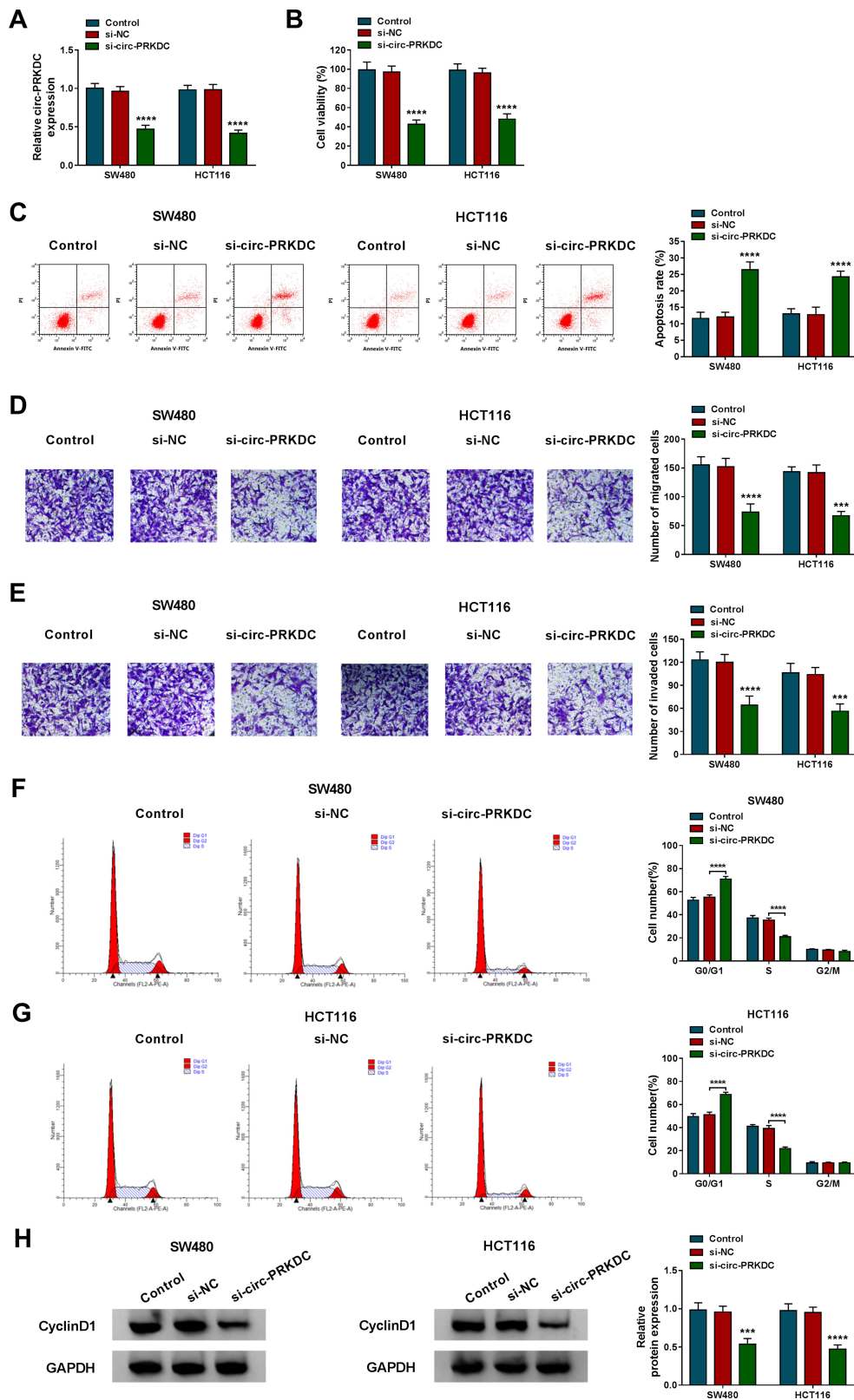


**Figure 2** Circ-PRKDC depletion inhibits proliferation, migration and invasion and promotes apoptosis in CRC cells. SW480 and HCT116 cells were introduced with si-NC or si-circ-PRKDC. **(A)** *Circ-PRKDC* expression was determined using qRT-PCR. **(B)** Cell viability was assessed using CCK-8 assay. **(C)** The apoptosis rate was measured via flow cytometry. **(D and E)** Cell migration and invasion were evaluated using transwell analysis. **(F and G)** Cell cycle was monitored using flow cytometry. **(H)** The protein level of CyclinD1 was examined using Western blot. \*\*\*\* $P < 0.0001$ , \*\*\* $P < 0.001$ .

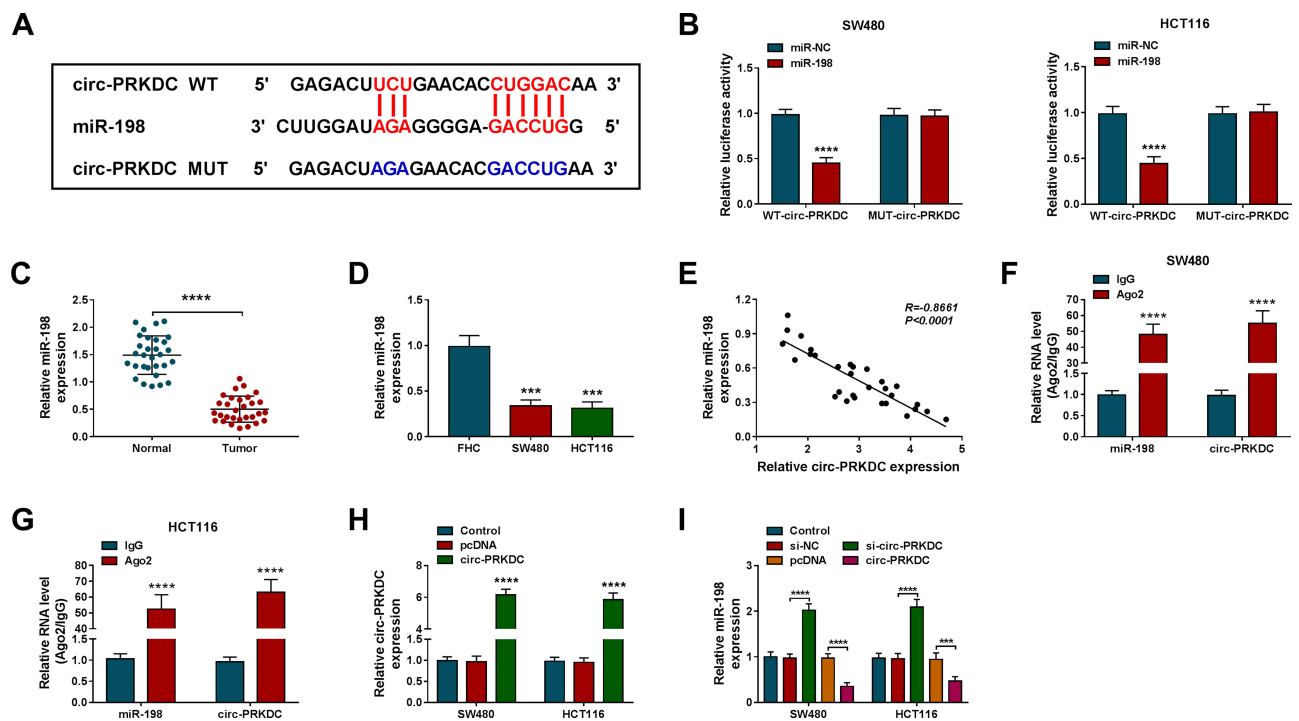


**Figure 3** Circ-PRKDC acts as a sponge for miR-198. **(A)** Circular RNA Interactome predicted that *circ-PRKDC* and *miR-198* had targeted binding sites. **(B)** Luciferase activity was detected in SW480 and HCT116 cells co-transfected with WT-*circ-PRKDC* or MUT-*circ-PRKDC* and miR-NC or miR-198. **(C)** *MiR-198* level was measured in CRC tissues and adjacent non-cancer tissues. **(D)** *MiR-198* level was detected in FHC, SW480 and HCT116 cells. **(E)** The correlation between *circ-PRKDC* and *miR-198* in CRC tissues was assessed using Spearman correlation coefficient. **(F and G)** The binding relationship between *circ-PRKDC* and *miR-198* was verified via RIP analysis. **(H)** *Circ-PRKDC* level was examined in SW480 and HCT116 cells transfected with pcDNA or *circ-PRKDC*. **(I)** *MiR-198* expression was measured in SW480 and HCT116 cells introduced with si-NC, si-*circ-PRKDC*, pcDNA or *circ-PRKDC*. \*\*\* $P < 0.001$ , \*\*\*\* $P < 0.0001$ .

and *miR-485-3p*) that were down-regulated in CRC. Next, the expression levels of four miRNAs were detected by qRT-PCR after *circ-PRKDC* knockdown. The results showed that the up-regulation of *miR-198* was the most significant, so we chose *miR-198* as the possible target of *circ-PRKDC* (Figure S2). The online database TargetScan suggested a shared sequence between *miR-198* and *DDR1* 3'UTR (Figure 5A). Dual-luciferase reporter assay showed that mature *miR-198* overtly decreased the luciferase activity of WT-*DDR1* 3'UTR reporter (Figure 5B). Compared to normal tissues, *DDR1* mRNA and protein levels were significantly elevated in CRC tissues (Figure 5C and D). Spearman correlation coefficient revealed that *miR-198* and *DDR1* had a negative correlation in CRC tissues (Figure 5E). Additionally, the mRNA and protein levels of *DDR1* in SW480 and HCT116 cells were remarkably higher than those in FHC cells (Figure 5F and G). Moreover, the binding relationship between *miR-198* and *DDR1* was verified by RIP assay, and the results exhibited that *miR-198* and *DDR1* were enriched in Ago2 group (Figure 5H and I). As shown in Figure 5J, the overexpression efficiency of *miR-198* was examined using qRT-PCR

assay. Besides, *miR-198* up-regulation restrained *DDR1* mRNA and protein expression, whereas *miR-198* knock-down had the opposite effect (Figure 5K–M). Thus, these data reflected that *miR-198* negatively targeted *DDR1*.

## DDR1 Up-Regulation Attenuates the Effect of miR-198 Overexpression on CRC Cell Progression

Firstly, *DDR1* expression was markedly increased in the *DDR1* group relative to the pcDNA group, indicating a significant overexpression efficiency (Figure 6A and B). To explore the effects of *miR-198* and *DDR1* on CRC cell growth, SW480 and HCT116 cells were transfected with miR-NC, miR-198, miR-198+pcDNA or miR-198+*DDR1*, respectively. As displayed in Figure 6C–F, augmentation of *miR-198* suppressed cell viability, migration and invasion, and triggered apoptosis in SW480 and HCT116 cells, while introduction of miR-198+*DDR1* partially abrogated these effects. Furthermore, overexpression of *DDR1* partially abated the promotion of *miR-198* up-regulation on cell cycle arrest (Figure 6G). Also, co-transfection with *miR-198* and *DDR1* partially alleviated the reduction of CyclinD1 level caused by

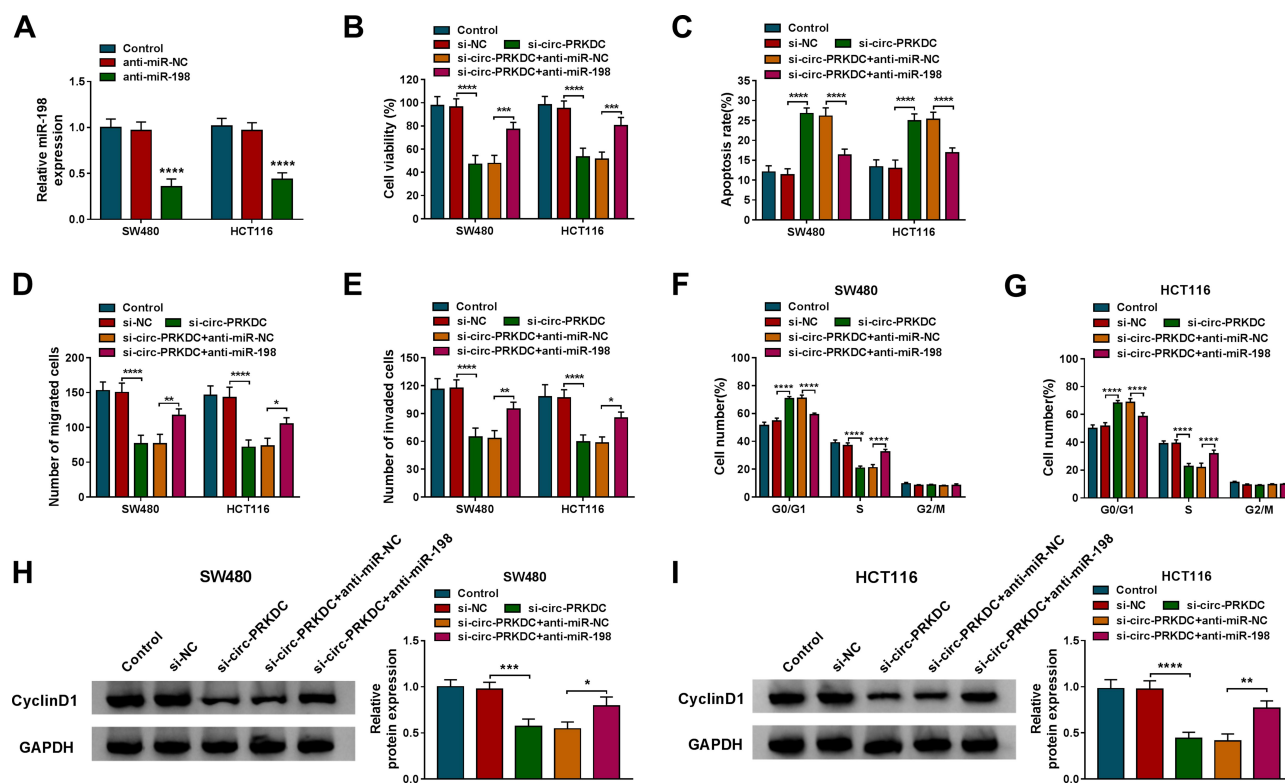


**Figure 4** Inhibition of miR-198 alleviates the effect of circ-PRKDC silencing on CRC cell progression. (A) The expression of miR-198 was measured in SW480 and HCT116 cells transfected with anti-miR-NC or anti-miR-198. Cell viability (B), apoptosis rate (C), migration (D), invasion (E), cell cycle (F and G) and CyclinD1 protein expression (H and I) were examined in SW480 and HCT116 cells transfected with si-NC, si-circ-PRKDC, si-circ-PRKDC+anti-miR-NC or si-circ-PRKDC+anti-miR-198. \* $P < 0.05$ , \*\* $P < 0.01$ , \*\*\* $P < 0.001$ , \*\*\*\* $P < 0.0001$ .

miR-198 overexpression (Figure 6H and I). These results indicated that miR-198 hindered CRC cell progression via targeting *DDR1*.

## Circ-PRKDC Regulates *DDR1* Expression via Sponging miR-198

We also investigated the interaction among *circ-PRKDC*, miR-198 and *DDR1* by detecting *DDR1* expression in SW480 and HCT116 cells after transfection. The results depicted that *DDR1* mRNA and protein levels were significantly reduced in the si-circ-PRKDC group compared with the si-NC group, whereas introduction of si-circ-PRKDC and anti-miR-198 undermined *circ-PRKDC* knockdown-induced decrease in *DDR1* expression (Figure 7A and B). These results indicated that *circ-PRKDC* sponged miR-198 to elevate *DDR1* expression.

## Silencing of Circ-PRKDC Inhibits Tumor Growth in vivo

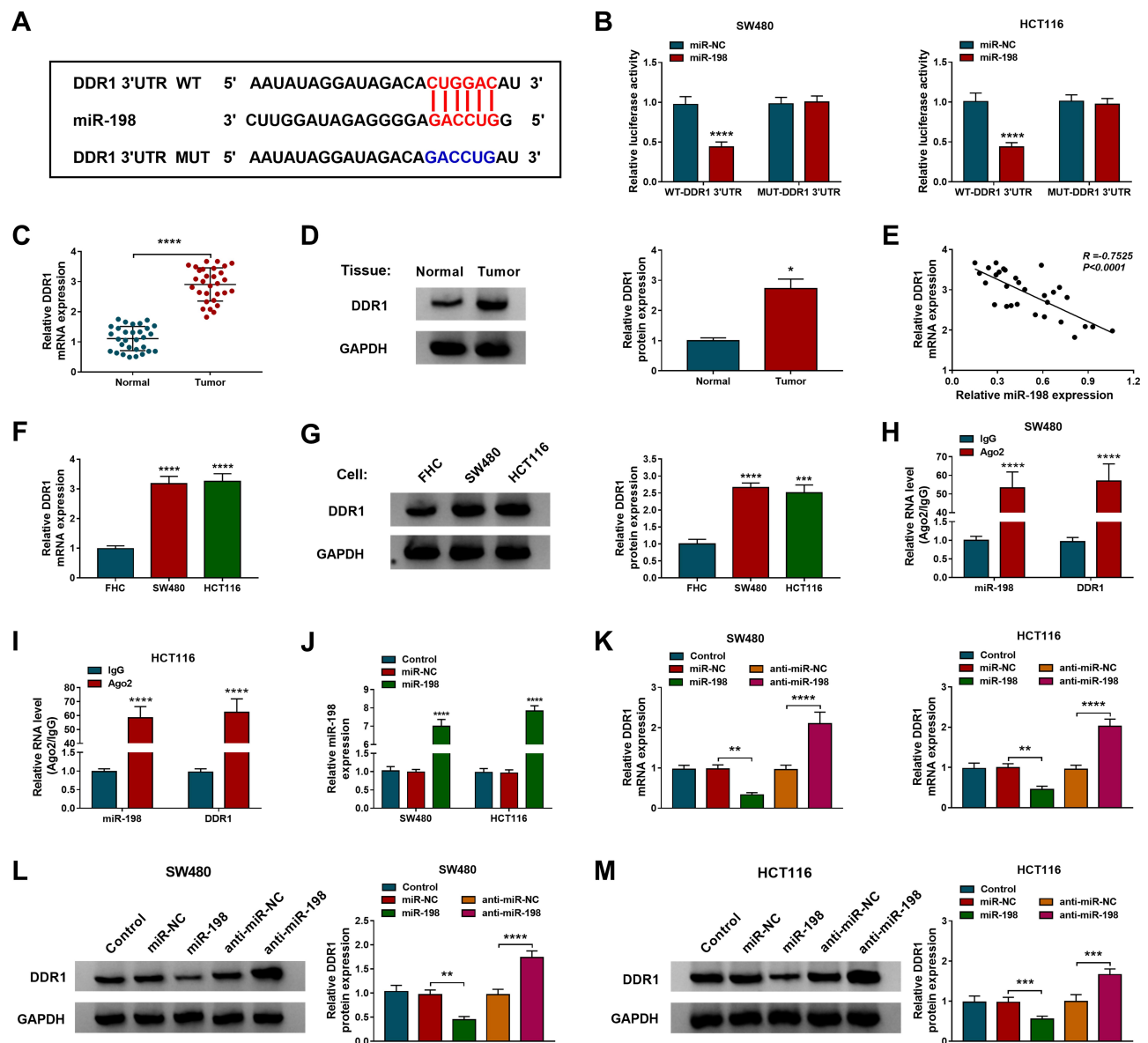
We used a xenograft mouse model to explore the role of *circ-PRKDC* in tumorigenesis in vivo. As exhibited in

Figure 8A and B, tumor volume was markedly reduced in the sh-circ-PRKDC group compared with the sh-NC group. Also, *circ-PRKDC* silencing significantly decreased tumor weight (Figure 8C). Moreover, the expression of *circ-PRKDC* and *DDR1* was significantly decreased, and miR-198 level was significantly elevated in the sh-circ-PRKDC group relative to the sh-NC group (Figure 8D and E). In addition, silencing of *circ-PRKDC* significantly reduced the expression of CyclinD1,  $\beta$ -catenin and c-Myc in xenograft tumors (Figure 8F). These data indicated that *circ-PRKDC* knockdown blocked tumor growth in vivo.

## Discussion

In recent years, circRNAs with high stability and tissue specificity are receiving increasing attention. Emerging evidence has manifested that circRNAs exert regulatory effects on biological functions, including proliferation, apoptosis and metastasis.<sup>28</sup> A growing number of abnormally expressed circRNAs occupy a vital position in the regulation of CRC development.<sup>10</sup> For example, *circ5615* triggered CRC cell proliferation and restrained cell cycle arrest via interacting with miR-149-5p to up-regulate *TNKS*.<sup>29</sup> *CircVAPA*





**Figure 5** DDR1 is a target of miR-198. **(A)** The predicted binding sites of miR-198 and DDR1 3'UTR were exhibited. **(B)** Luciferase activity was detected in SW480 and HCT116 cells introduced with WT-DDR1 3'UTR or MUT-DDR1 3'UTR and miR-NC or miR-198. **(C and D)** The mRNA and protein levels of *DDR1* were measured in CRC tissues and normal tissues. **(E)** The correlation between miR-198 and *DDR1* in CRC tissues was tested via Spearman correlation analysis. **(F and G)** *DDR1* mRNA and protein levels were examined in FHC, SW480 and HCT116 cells. **(H and I)** RIP assay was used to confirm the relationship between miR-198 and *DDR1*. **(J)** Expression of miR-198 was detected in SW480 and HCT116 cells transfected with miR-NC or miR-198. **(K–M)** *DDR1* mRNA and protein levels were measured in SW480 and HCT116 cells transfected with miR-NC, miR-198, anti-miR-NC or anti-miR-198. \* $P < 0.05$ , \*\* $P < 0.01$ , \*\*\*\* $P < 0.0001$ , \*\*\*\* $P < 0.0001$ .

contributed to CRC cell growth and glycolysis by directly combining with *miR-125a* to release *CREB5*.<sup>30</sup> In this research, we determined that silenced *circ-PRKDC* suppressed CRC cell proliferation, migration and invasion, and triggered apoptosis. Subsequently, we selected *miR-198* as a possible target for *circ-PRKDC* based on bioinformatics analysis.

Compelling evidence has illuminated that circRNAs serve as a competing endogenous RNA (ceRNA) to modulate gene expression, thereby affecting a range of

biological processes.<sup>31</sup> A previous report suggested that *miR-198* is one of the top 10 miRNAs down-regulated in CRC tumor stroma with synchronized liver metastasis.<sup>32</sup> Besides, more and more studies have confirmed that *miR-198* is a tumor-inhibiting factor in various tumors. In breast cancer, *miR-198* attenuated the malignancy of tumor by decreasing *CDCP1* expression.<sup>33</sup> In gastric cancer, *miR-198* restrained tumorigenesis via targeting *FGFR1* and had better efficacy in combination with cisplatin.<sup>34</sup> Furthermore, Wang

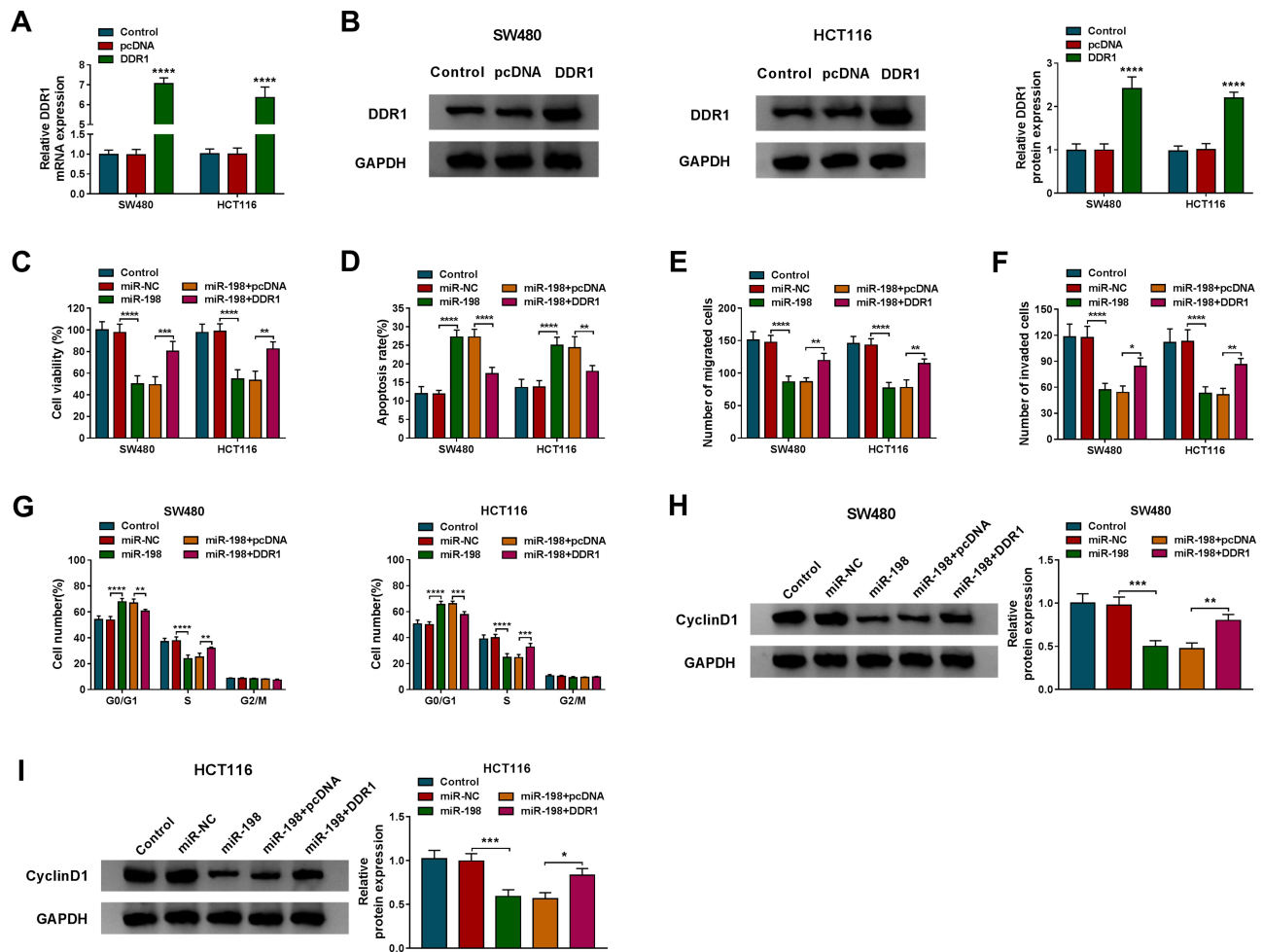


**Figure 6** DDR1 up-regulation attenuates the effect of miR-198 overexpression on CRC cell progression. (A and B) After SW480 and HCT116 cells were introduced with pcDNA or DDR1, *DDR1* mRNA and protein levels were determined using qRT-PCR and Western blot. Cell viability (C), apoptosis rate (D), migration (E), invasion (F), cell cycle (G) and CyclinD1 protein level (H and I) were detected in SW480 and HCT116 cells transfected with miR-NC, miR-198, miR-198+pcDNA or miR-198+DDR1. \* $P < 0.05$ , \*\* $P < 0.01$ , \*\*\* $P < 0.001$ , \*\*\*\* $P < 0.0001$ .

et al unveiled that low *miR-198* expression was closely related to poor overall survival and up-regulation of *miR-198* blocked CRC cell growth by repressing *FUT8*.<sup>20</sup> In the present research, we first evidenced that *circ-PRKDC* might be a ceRNA for *miR-198* and expedited CRC development via sponging *miR-198*.

To further clarify the potential mechanism of *circ-PRKDC*, we predicted the possible target genes of *miR-198*. Mounting evidence has manifested that miRNAs influence gene expression by pairing with 3'UTR of mRNAs.<sup>35</sup> Plenty of investigations have revealed that *DDR1* acts as an oncogene by regulating cell processes such as growth and metastasis in various tumors.<sup>36</sup> For example, Zhong et al disclosed that *DDR1* augmentation induced tumorigenesis via hindering antitumor immunity in breast cancer.<sup>37</sup> Chou et al

found that suppression of *DDR1* restrained cell growth and accelerated apoptosis in oral cancer.<sup>38</sup> Moreover, the previous study indicated that *DDR1* silencing impeded tumor progression in CRC by interacting with *miR-199a-5p*.<sup>39</sup> Our research unearthed that *miR-198* targeted *DDR1* to inhibit CRC cell progression.

In short, these findings demonstrated that *circ-PRKDC* aggravated the malignancy of CRC via modulating *miR-198/DDR1* regulatory axis. We revealed a new ceRNA mechanism, which might provide a novel therapeutic strategy for CRC. However, the limitation of this study is that the sample size is too small. It is necessary to expand the sample size and further study the clinical significance of *circ-PRKDC* in CRC.

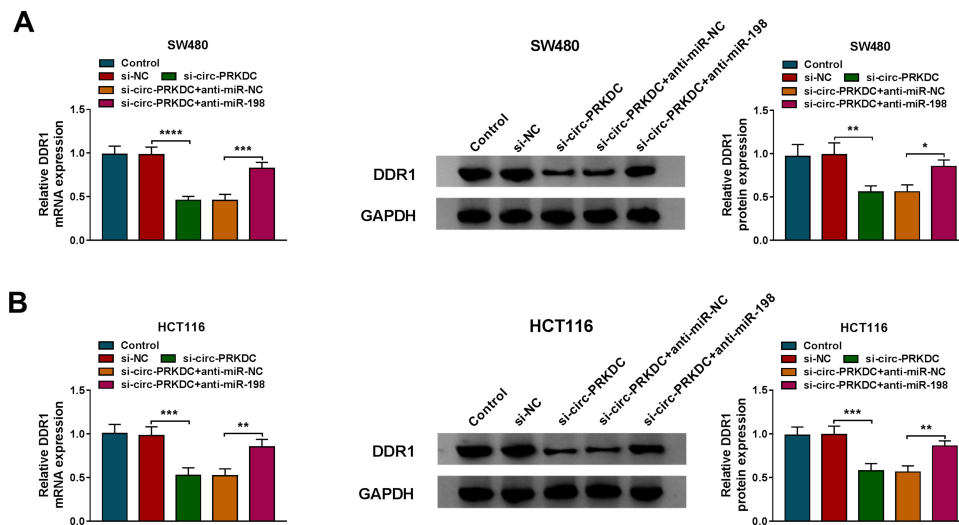


**Figure 7** Circ-PRKDC regulates DDR1 expression via sponging miR-198. (A and B) The mRNA and protein levels of *DDR1* were measured in SW480 and HCT116 cells introduced with si-NC, si-circ-PRKDC, si-circ-PRKDC+anti-miR-NC or si-circ-PRKDC+anti-miR-198. \* $P < 0.05$ , \*\* $P < 0.01$ , \*\*\* $P < 0.001$ , \*\*\*\* $P < 0.0001$ .

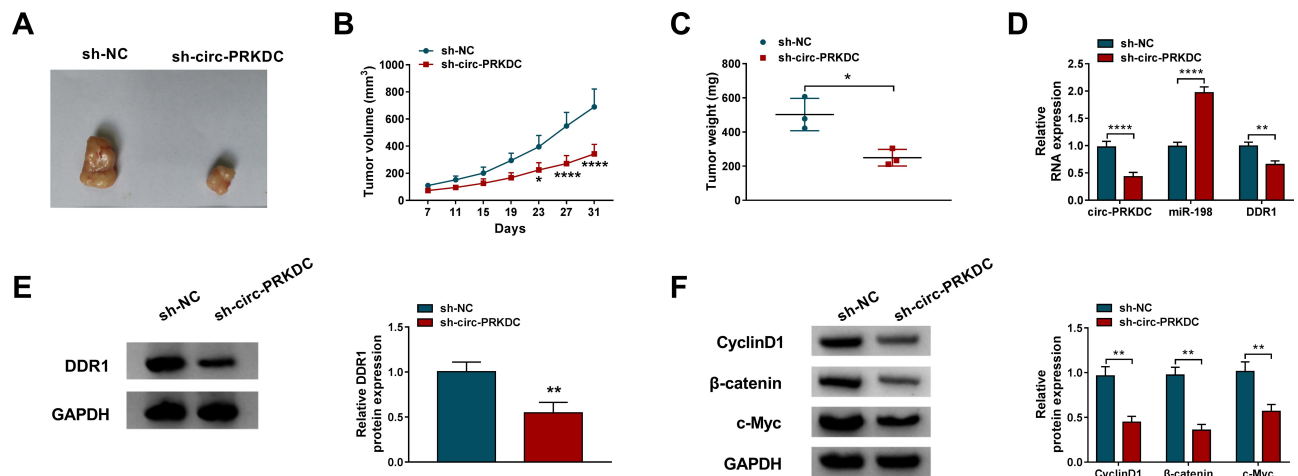


**Figure 8** Silencing of circ-PRKDC inhibits tumor growth in vivo. SW480 cells transfected with sh-NC or sh-circ-PRKDC were subcutaneously injected into nude mice. (A and B) Tumor volume was measured every 4 days. (C) After the mice were killed, the xenograft tumors were weighed. (D and E) The levels of *circ-PRKDC*, *miR-198* and *DDR1* in xenograft tumors were tested using qRT-PCR or Western blot. (F) The levels of CyclinD1,  $\beta$ -catenin and c-Myc in xenograft tumors were measured by Western blot. \* $P < 0.05$ , \*\* $P < 0.01$ , \*\*\* $P < 0.0001$ .

## Highlights

1. *Circ-PRKDC* level was enhanced in CRC tissues and cells.
2. *Circ-PRKDC* silencing inhibited CRC cell progression.
3. *Circ-PRKDC* promoted CRC progression via *miR-198/DDR1* axis.
4. *Circ-PRKDC* knockdown blocked tumor growth in vivo.

## Funding

This study was supported by National Science Foundation for Young Scientists of China Grant No. 81903268.

## Disclosure

The authors declare that they have no financial or non-financial conflicts of interest for this work.

## References

1. Dekker E, Tanis PJ, Vleugels JLA, Kasi PM, Wallace MB. Colorectal cancer. *Lancet*. 2019;394(10207):1467–1480. doi:10.1016/S0140-6736(19)32319-0
2. Bray F, Ferlay J, Soerjomataram I, Siegel RL, Torre LA, Jemal A. Global cancer statistics 2018: GLOBOCAN estimates of incidence and mortality worldwide for 36 cancers in 185 countries. *CA Cancer J Clin*. 2018;68(6):394–424. doi:10.3322/caac.21492

3. Brenner H, Kloor M, Pox CP. Colorectal cancer. *Lancet*. 2014;383(9927):1490–1502. doi:10.1016/S0140-6736(13)61649-9
4. Katona BW, Weiss JM. Chemoprevention of colorectal cancer. *Gastroenterology*. 2020;158(2):368–388. doi:10.1053/j.gastro.2019.06.047
5. Wolpin BM, Mayer RJ. Systemic treatment of colorectal cancer. *Gastroenterology*. 2008;134(5):1296–1310. doi:10.1053/j.gastro.2008.02.098
6. Qian L, Yu S, Chen Z, Meng Z, Huang S, Wang P. The emerging role of circRNAs and their clinical significance in human cancers. *Biochim Biophys Acta Rev Cancer*. 2018;1870(2):247–260.
7. Cui X, Wang J, Guo Z, et al. Emerging function and potential diagnostic value of circular RNAs in cancer. *Mol Cancer*. 2018;17(1):123. doi:10.1186/s12943-018-0877-y
8. Wang N, Lu K, Qu H, et al. CircRBM33 regulates IL-6 to promote gastric cancer progression through targeting miR-149. *Biomed Pharmacother*. 2020;125:109876. doi:10.1016/j.biopha.2020.109876
9. Liu T, Ye P, Ye Y, Lu S, Han B. Circular RNA hsa\_circRNA\_002178 silencing retards breast cancer progression via microRNA-328-3p-mediated inhibition of COL1A1. *J Cell Mol Med*. 2020;24(3):2189–2201. doi:10.1111/jcmm.14875
10. Hao S, Cong L, Qu R, Liu R, Zhang G, Li Y. Emerging roles of circular RNAs in colorectal cancer. *Oncotargets Ther*. 2019;12:4765–4777. doi:10.2147/OTT.S208235
11. Jin C, Wang A, Liu L, Wang G, Li G. Hsa\_circ\_0136666 promotes the proliferation and invasion of colorectal cancer through miR-136/SH2B1 axis. *J Cell Physiol*. 2019;234(5):7247–7256. doi:10.1002/jcp.27482
12. Chen H, Pei L, Xie P, Guo G. Circ-PRKDC contributes to 5-fluorouracil resistance of colorectal cancer cells by regulating miR-375/FOXO1 axis and Wnt/beta-catenin pathway. *Oncotargets Ther*. 2020;13:5939–5953. doi:10.2147/OTT.S253468
13. Liu LH, Tian QQ, Liu J, Zhou Y, Yong H. Upregulation of hsa\_circ\_0136666 contributes to breast cancer progression by sponging miR-1299 and targeting CDK6. *J Cell Biochem*. 2019;120(8):12684–12693. doi:10.1002/jcb.28536
14. Chen Y, Gao DY, Huang L. In vivo delivery of miRNAs for cancer therapy: challenges and strategies. *Adv Drug Deliv Rev*. 2015;81:128–141. doi:10.1016/j.addr.2014.05.009
15. Di Leva G, Garofalo M, Croce CM. MicroRNAs in cancer. *Annu Rev Pathol*. 2014;9:287–314. doi:10.1146/annurev-pathol-012513-104715
16. Shirmohamadi M, Eghbali E, Najjary S, et al. Regulatory mechanisms of microRNAs in colorectal cancer and colorectal cancer stem cells. *J Cell Physiol*. 2020;235(2):776–789. doi:10.1002/jcp.29042
17. Hong YG, Xin C, Zheng H, et al. miR-365a-3p regulates ADAM10-JAK-STAT signaling to suppress the growth and metastasis of colorectal cancer cells. *J Cancer*. 2020;11(12):3634–3644. doi:10.7150/jca.42731
18. Li J, Peng W, Yang P, et al. MicroRNA-1224-5p inhibits metastasis and epithelial-mesenchymal transition in colorectal cancer by targeting SP1-mediated NF-kappaB signaling pathways. *Front Oncol*. 2020;10:294. doi:10.3389/fonc.2020.00294
19. Sun N, Zhang L, Zhang C, Yuan Y. miR-144-3p inhibits cell proliferation of colorectal cancer cells by targeting BCL6 via inhibition of Wnt/beta-catenin signaling. *Cell Mol Biol Lett*. 2020;25:19. doi:10.1186/s11658-020-00210-3
20. Wang M, Wang J, Kong X, et al. MiR-198 represses tumor growth and metastasis in colorectal cancer by targeting fucosyl transferase 8. *Sci Rep*. 2014;4:6145. doi:10.1038/srep06145
21. Li LX, Lam IH, Liang FF, et al. MiR-198 affects the proliferation and apoptosis of colorectal cancer through regulation of ADAM28/JAK-STAT signaling pathway. *Eur Rev Med Pharmacol Sci*. 2019;23(4):1487–1493.
22. Leitinger B. Discoidin domain receptor functions in physiological and pathological conditions. *Int Rev Cell Mol Biol*. 2014;310:39–87.
23. Yeh YC, Lin HH, Tang MJ. Dichotomy of the function of DDR1 in cells and disease progression. *Biochim Biophys Acta Mol Cell Res*. 2019;1866(11):118473. doi:10.1016/j.bbmr.2019.04.003
24. Chen YL, Tsai WH, Ko YC, et al. Discoidin domain receptor-1 (DDR1) is involved in angiolymphatic invasion in oral cancer. *Cancers (Basel)*. 2020;12(4):841. doi:10.3390/cancers12040841
25. Wu A, Chen Y, Liu Y, Lai Y, Liu D. miR-199b-5p inhibits triple negative breast cancer cell proliferation, migration and invasion by targeting DDR1. *Oncol Lett*. 2018;16(4):4889–4896.
26. Vella V, Nicolosi ML, Cantafio P, et al. DDR1 regulates thyroid cancer cell differentiation via IGF-2/IR-A autocrine signaling loop. *Endocr Relat Cancer*. 2019;26(1):197–214. doi:10.1530/ERC-18-0310
27. Sirvent A, Lafitte M, Roche S. DDR1 inhibition as a new therapeutic strategy for colorectal cancer. *Mol Cell Oncol*. 2018;5(4):e1465882. doi:10.1080/23723556.2018.1465882
28. Qu S, Liu Z, Yang X, et al. The emerging functions and roles of circular RNAs in cancer. *Cancer Lett*. 2018;414:301–309. doi:10.1016/j.canlet.2017.11.022
29. Ma Z, Han C, Xia W, et al. circ5615 functions as a ceRNA to promote colorectal cancer progression by upregulating TNKS. *Cell Death Dis*. 2020;11(5):356. doi:10.1038/s41419-020-2514-0
30. Zhang X, Xu Y, Yamaguchi K, et al. Circular RNA circVAPA knock-down suppresses colorectal cancer cell growth process by regulating miR-125a/CREB5 axis. *Cancer Cell Int*. 2020;20:103.
31. Zhong Y, Du Y, Yang X, et al. Circular RNAs function as ceRNAs to regulate and control human cancer progression. *Mol Cancer*. 2018;17(1):79.
32. Murakami T, Kikuchi H, Ishimatsu H, et al. Tenascin C in colorectal cancer stroma is a predictive marker for liver metastasis and is a potent target of miR-198 as identified by microRNA analysis. *Br J Cancer*. 2017;117(9):1360–1370. doi:10.1038/bjc.2017.291
33. Hu Y, Tang Z, Jiang B, Chen J, Fu Z. miR-198 functions as a tumor suppressor in breast cancer by targeting CUB domain-containing protein 1. *Oncol Lett*. 2017;13(3):1753–1760. doi:10.3892/ol.2017.5673
34. Gu J, Li X, Li H, Jin Z, Jin J. MicroRNA-198 inhibits proliferation and induces apoptosis by directly suppressing FGFR1 in gastric cancer. *Biosci Rep*. 2019;39(6). doi:10.1042/BSR20181258
35. Zhang Y, Wang Z, Gemeinhart RA. Progress in microRNA delivery. *J Control Release*. 2013;172(3):962–974. doi:10.1016/j.jconrel.2013.09.015
36. Borza CM, Pozzi A. Discoidin domain receptors in disease. *Matrix Biol*. 2014;34:185–192. doi:10.1016/j.matbio.2013.12.002
37. Zhong X, Zhang W, Sun T. DDR1 promotes breast tumor growth by suppressing antitumor immunity. *Oncol Rep*. 2019;42(6):2844–2854.
38. Chou ST, Peng HY, Mo KC, et al. MicroRNA-486-3p functions as a tumor suppressor in oral cancer by targeting DDR1. *J Exp Clin Cancer Res*. 2019;38(1):281. doi:10.1186/s13046-019-1283-z
39. Hu Y, Liu J, Jiang B, et al. MiR-199a-5p loss up-regulated DDR1 aggravated colorectal cancer by activating epithelial-to-mesenchymal transition related signaling. *Dig Dis Sci*. 2014;59(9):2163–2172. doi:10.1007/s10620-014-3136-0

**Cancer Management and Research**

Dovepress

**Publish your work in this journal**

Cancer Management and Research is an international, peer-reviewed open access journal focusing on cancer research and the optimal use of preventative and integrated treatment interventions to achieve improved outcomes, enhanced survival and quality of life for the cancer patient.

The manuscript management system is completely online and includes a very quick and fair peer-review system, which is all easy to use. Visit <http://www.dovepress.com/testimonials.php> to read real quotes from published authors.

Submit your manuscript here: <https://www.dovepress.com/cancer-management-and-research-journal>